Topological Change of the Fermi Surface in Ternary Iron Pnictides with Reduced c/a Ratio: A de Haas–van Alphen Study of $CaFe_2P_2$

Amalia I. Coldea,[1] C. M. J. Andrew,[1] J. G. Analytis,[2,3] R. D. McDonald,[4] A. F. Bangura,[1] J.-H. Chu,[2,3] I. R. Fisher,[2,3] and A. Carrington[1]

[1]*H. H. Wills Physics Laboratory, University of Bristol, Tyndall Avenue, Bristol, BS8 1TL, United Kingdom*
[2]*Stanford Institute for Materials and Energy Sciences, SLAC National Accelerator Laboratory, 2575 Sand Hill Road, Menlo Park, California 94025, USA*
[3]*Geballe Laboratory for Advanced Materials and Department of Applied Physics, Stanford University, Stanford, California 94305-4045, USA*
[4]*Los Alamos National Laboratory, Los Alamos, New Mexico 87545, USA*

(Received 20 May 2009; published 10 July 2009)

We report a de Haas–van Alphen effect study of the Fermi surface of $CaFe_2P_2$ using low-temperature torque magnetometry up to 45 T. This system is a close structural analog of the collapsed tetragonal nonmagnetic phase of $CaFe_2As_2$. We find the Fermi surface of $CaFe_2P_2$ to differ from other related ternary phosphides in that its topology is highly dispersive in the c axis, being three dimensional in character and with identical mass enhancement on both electron and hole pockets ($\sim$1.5). This suggests that when the bonding between pnictogen layers becomes important nesting conditions are not fulfilled.

DOI: 10.1103/PhysRevLett.103.026404 PACS numbers: 71.18.+y, 74.25.Jb, 74.70.−b

The nature of the Fermi surface dimensionality and its proximity to nesting in the iron-pnictide superconductors is at the core of understanding the mechanism of superconductivity. An important finding is that under *hydrostatic* pressure, $BaFe_2As_2$ and $SrFe_2As_2$ [1] superconduct whereas $CaFe_2As_2$ does not [2]. Instead it undergoes a structural transition to a phase with a much reduced c-axis length which is known as the ''collapsed tetragonal'' (CT) state. If pressure is applied using a nonhydrostatic medium $CaFe_2As_2$ does become superconducting [1,3]. This suggests that small uniaxial pressure components stabilize the superconductivity in $CaFe_2As_2$. Understanding why this happens in these materials and whether the Fermi surface nesting or the strong coupling with the lattice are the relevant parameters will be important for understanding the origin of superconductivity in iron pnictides.

$CaFe_2As_2$ has three distinct magnetic and structural phases. Like many other iron arsenides, at zero pressure, the high temperature tetragonal state becomes orthorhombic and antiferromagnetically ordered below $T_N \simeq 170$ K. At low temperatures under a pressure of 0.35 GPa there is a transition to the CT state in which there is a $\sim$10% decrease in the c-axis lattice parameter and a $\sim$2% increase in the a-axis [4]. Recent band structure calculations [5,6] suggest that these phase transitions have a dramatic effect on the Fermi surface. In the high temperature tetragonal phase the Fermi surface is predicted to be similar to the other 122 pnictide consisting of two strongly warped electron cylinders at the Brillouin zone corners and hole cylinders at the center of the zone (Γ). However, in the CT state the calculated Fermi surface suffers a major topological change; the two electron cylinders at the zone corners transform into a single warped cylinder whereas the hole cylinders become a large three-dimensional sheet.

The Fermi surface of many iron-pnictides have been extensively studied by angle resolved photoemission spectroscopy, however, the CT phase of $CaFe_2As_2$ is inaccessible to this technique due of the high pressures involved. Quantum oscillation (QO) studies have the advantage of probing precisely the bulk three-dimensional Fermi surface; these studies have been performed in the antiferromagnetically ordered phase of the iron-arsenides [7] but the tetragonal superconducting phase cannot be accessed because of the high values of the upper critical field ($\sim$100 T). Although QO studies are possible under high pressure, these measurements are technically very challenging. One route to provide an insight into the Fermi surface properties of the iron-arsenides is to study the analogous nonmagnetic phosphide materials. These materials have almost identical calculated Fermi surfaces to the arsenides in their nonmagnetic state but are either nonsuperconducting or have a low T_c (and low H_{c2}) and single crystals can be grown with very high purity making them ideal for QO studies. Quantum oscillations have been measured in superconducting LaFePO [8] (which is analogous to the nonmagnetic ''1111'' arsenides, e.g., LaFeAsO) and $SrFe_2P_2$ [9] (which is a structural analogue to the nonmagnetic tetragonal ''122'' arsenides).

Here we report a de Haas–van Alphen effect study of the Fermi surface of $CaFe_2P_2$ which is a very close structural analogue of the CT phase of $CaFe_2As_2$. The isoelectric substitution of As with P does not change the number of Fe $3d$ electrons, but enhances P-P hybridization causing the lattice to contract in the c direction. Consequently the interlayer P-P distance approaches the molecular bond length [10], just as the As-As distance does in the CT phase [11]. We show experimentally that the Fermi surface of $CaFe_2P_2$ is different from the multiband electron-hole

structure found in $SrFe_2P_2$ [9] and other pnictides, and is formed of a single warped cylinder and a large three-dimensional hole sheet. We find a isotropic mass enhancements on the electron and hole sheets (~1.5).

High quality single crystals of $CaFe_2P_2$ were grown from a Sn flux similar to previous reports [9]. The residual resistivity ratio $\rho(300\ \mathrm{K})/\rho(1.8\ \mathrm{K})$ was measured to be greater than 120. Torque magnetometry was performed using piezoresistive microcantilevers in high fields 18 T in Bristol (sample B) and 45 T (sample A) at the NHFML, Tallahassee. We compare our data with the predictions of bandstructure calculations which we performed using an augmented plane wave plus local orbital method (WIEN2K code) [12] with the experimentally determined lattice parameters and internal positions [13].

Figure 1(a) shows the oscillatory part of raw torque signal for a $CaFe_2P_2$ crystal up to 45 T. The fast Fourier transform (FFT) for several other orientations as the field is rotated from $B \parallel c$ ($\theta = 0$) towards $B \parallel a$ ($\theta = 90°$) is shown in Fig. 1(b). The FFT frequencies F of oscillatory torque data (in the $1/B$ domain) are related to extremal Fermi surface areas by $F = (\hbar/2\pi e)A_k$. Close to $B \parallel c$ the strongest amplitude peak (α_1) is at 4.35 kT and we also

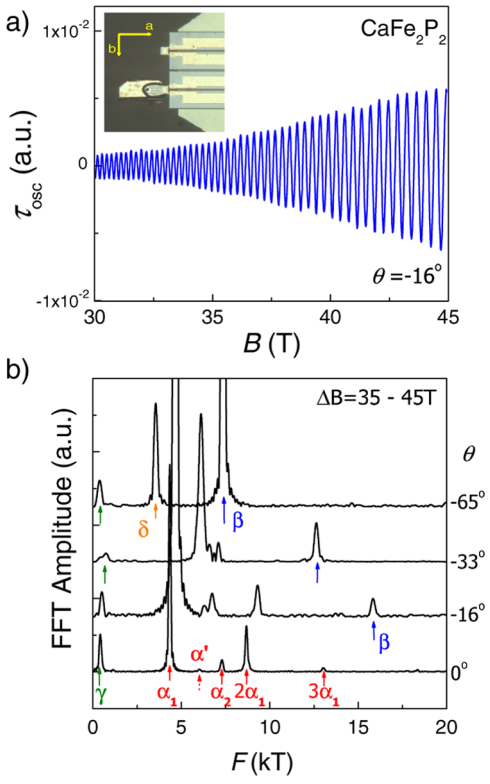

FIG. 1 (color online). (a) Oscillatory part of torque at $T = 0.4$ K for a single crystal of $CaFe_2P_2$ (sample A). The inset shows sample A attached to a piezocantilever. (b) The Fourier transform spectra showing the evolution of the extremal areas of the Fermi surface with the field angle, θ. The positions of different pockets, α_1, α_2, β, γ, δ and harmonics ($2\alpha_1$, $3\alpha_1$) as well as a weak peak, α' are indicated by arrows.

observe several harmonics of α_1 [see Fig. 1(b)]; we can distinguish a frequency $\alpha_2 \sim 7.3$ kT and a tiny feature α' at 6 kT [15]. A small pocket γ is observed at ~420 T; at higher angles ($\theta = 15°$) the amplitude of another frequency, β, becomes significant and the position of this peak varies strongly with increasing angle. When we rotate close to $B||a$ a strong amplitude signal, δ, corresponding to an extremal area of 3.2 kT is found.

The angular dependence of the observed dHvA frequencies allows us to identify the shape of the Fermi surface sheets from which they originate (see Fig. 2). Rotating away from $B \parallel c$ the α_1 and α_2 orbits display a much stronger angular variation compared to extremal orbits on a simple cylinder with a weak k_z dispersion ($F(\theta) \sim 1/\cos\theta$) [8]. This suggests that these orbits originate from a strongly warped cylindrical Fermi surface [15]. The size of the β orbit changes dramatically with θ suggesting that this Fermi surface sheet has an prolate ellipsoidal shape with a maximum at $\theta = 0°$. The α orbits are well reproduced in both samples, but the β orbit was only observed in sample A in much higher fields (up to 45 T). This can be explained as the impurity damping of the dHvA signal is proportional to $\exp(-k_F/(\ell B))$ so that higher field are needed to see the larger β orbit ($k_F \propto \sqrt{F}$) for the same mean free path (ℓ).

We now compared the experimental data in $CaFe_2P_2$ to the predictions of the band structure calculations.

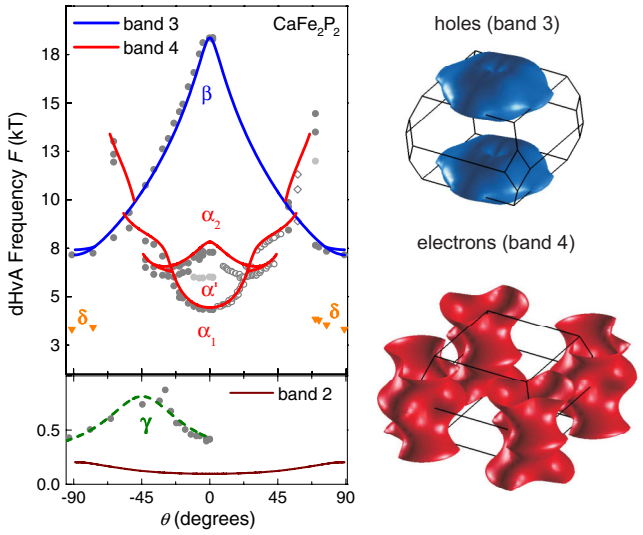

FIG. 2 (color online). Angle dependence of all observed frequencies compared with the band structure predictions (solid lines). Different symbols correspond to sample A (filled circles) and sample B (open circles). Solid grey points indicate the position of very weak features. The bottom panel shows an expanded low frequency scale for the γ pocket and the dotted line is a guide to the eye. The calculated Fermi surface of $CaFe_2P_2$ is also shown. The solid lines delimits the Brillouin zone and the Fermi surface sheets are represented in an extended zone.

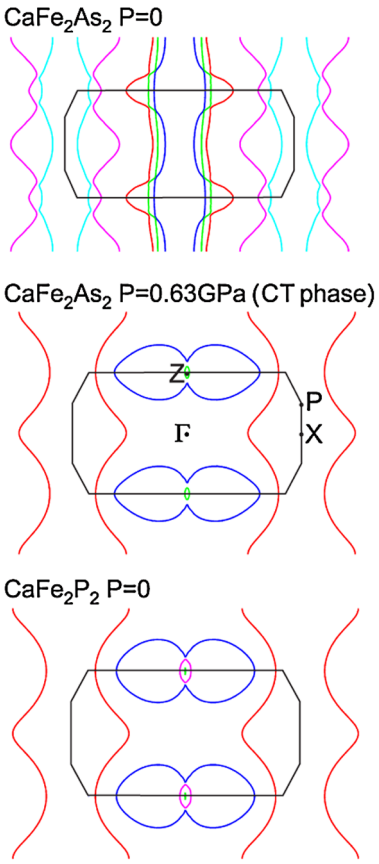

FIG. 3 (color online). Comparison of the calculated Fermi surface topology of $CaFe_2As_2$ (tetragonal phase), $CaFe_2As_2$ (CT phase) and $CaFe_2P_2$. Slices through the center of the Brillouin zone (solid lines) in the (110) plane are shown.

The Fermi surface (see Figs. 2 and 3) is quasi-three-dimensional and is composed of a large hole sheet in the form of a flat pillow at the top of the zone whereas the electron sheets are strongly distorted quasi-two-dimensional cylinders centered on the zone corners. There are also two tiny hole pockets centered at Z (see the bottom panel of Fig. 3) containing only $\sim$0.008 holes compared with the large hole and electron sheets which each contains $\sim$0.41 holes/electrons; if the P position is optimized in the calculation (by minimizing the total energy, $z_P = 0.3890$) they disappear.

Figure 2 shows good agreement between data and calculation in the case of the β frequency which corresponds to cross sections on the hole sheet (band 3) and the α_1 and α_2 frequencies which correspond to the minimum and maximal extremal areas of the strongly warped electron cylinder (band 4) (the degree of warping is roughly $\Delta F/F \sim 50\%$ in $CaFe_2P_2$ as compared with $\sim$23% in $SrFe_2P_2$ [9]). Further weak in-plane or interplane dispersion on either hole or electron sheets could give rise to additional branches, not predicted by our calculations. This could explain the origin of the δ branch, which is observed within $\sim 25°$ of $\theta = 90°$ ($B \parallel a$) (Fig. 2); it may also account for the small shift found for α_2 as well as the presence of the weak feature at α'. It is worth emphasizing that the agreement between data and calculations ($\pm$10 meV) for the main sheets is good in contrast to our findings for LaFePO and $SrFe_2P_2$ [8,9] where rigid band shift of up to 100 meV were needed to bring the band structure into agreement with experiment.

Any small band shifts would mainly affect the small pockets of the Fermi surface centered at the Z point, as stated earlier. For example, by shifting the hole bands down the tiny pockets at the Z point disappear and the large hole pillow transforms into a large torroid; this may give rise to the δ branch (which is about half the size of the β orbit) when to $B \parallel a$ (see bottom panel of Fig. 3). The γ frequency increases to about $\theta = 42(3)°$ and then decrease suggesting that it has a short closed cylinder shape (see Fig. 2). By shifting the hole bands up (by $\sim$40 meV) the small 3D pocket centered at the Z point (band 2) could be assigned to the γ branch (Fig. 3). Alternatively, γ which has a low effective mass ($m^* = 0.4m_e$) could originate from an Sn impurity phase which has orbits with similar frequencies and masses [16], but x-ray diffraction does not identify any Sn impurities at the level of $\sim$1%. In any case this pocket, γ, accounts for only a tiny fraction of holes ($\sim$0.03) and we believe it is unlikely to play any major role.

Figure 3 shows a comparison between the Fermi surface of $CaFe_2As_2$ in the tetragonal phase ($c/a = 2.98$), $CaFe_2As_2$ in the CT phase ($c/a = 2.66$ at $P = 0.63$ GPa) and $CaFe_2P_2$ ($c/a = 2.59$). As mentioned before, it is clear that there is a remarkable similarity between $CaFe_2P_2$ and the CT phase of $CaFe_2As_2$. Thus in $CaFe_2As_2$ applying *chemical pressure* (by the isoelectronic substitution of As by P) is equivalent to *applied hydrostatic pressure*, as found in other ternary pnictides [17]. This state of reduced c/a ratio has a different Fermi surface topology compared to $CaFe_2As_2$ or $SrFe_2P_2$ ($c/a = 3.03$). Yildirim [11] has argued that the CT phase of $CaFe_2As_2$ occurs when, by reducing the Fe moment, the Fe-As bonding weakens and the (inter and intraplanar) As-As bonding gets stronger causing the significant strong reduction in the c axis [4]. Similarly, in nonmagnetic phosphides, the reduction in the c axis (or the c/a ratio) results in an increase P-P hybridization between pnictogen ions along the c direction (close to the single bond distance) [10]. The spacer between the iron layers (Sr or Ba) limits the degree of this hybridization between layers and such a state with strong pnictogen bonding is unlikely to occur [6,17].

The effective masses, m^*, of $CaFe_2P_2$ for each Fermi surface orbit extracted from the temperature dependence of the dHvA signals, using the conventional Lifshitz-Kosevich formula [18], are shown in Table I and compared to the corresponding band structure values. The masses for the electron and hole sheets are enhanced by the same factor of $\sim$1.5 in contrast to the sheet dependent variation

TABLE I. Experimental and calculated Fermi surface parameters of $CaFe_2P_2$ close to $\theta = 0°$ ($B \parallel c$) similar to those predicted for $CaFe_2As_2$ in the CT phase [5].

	Experiment			Calculations			
	F (kT)	$\frac{m^*}{m_e}$	ℓ (nm)	Orbit	F (kT)	$\frac{m_b}{m_e}$	$\frac{m^*}{m_b}$
$\alpha_1(e)$	4.347	2.05(4)	190	$4_{\min}$	4.439	1.38	1.49(3)
$\alpha_2(e)$	7.295	3.48(7)	71	$4_{\max}$	7.837	2.40	1.45(3)
$\beta(h)$	18.360	4.0(2)	86	$3_{\min}$	18.407	2.65	1.51(8)

of the enhancement observed recently in $SrFe_2P_2$. By comparing the quasiparticle enhancement on the electron sheets (which have the largest mean free path and often match better to the band structure calculations being less sensitive to structural changes compared with the hole pockets) we observe that in LaFePO the average enhancement is 2.38 (2.2 for inner and 2.54 for outer pocket) [8] whereas in $SrFe_2P_2$ is 1.85 (1.6 for inner and 2.1 for the outer electron sheet) [9]. The conventional electron-phonon coupling, $\lambda_{e-\mathrm{ph}}$, in the CT phase of $CaFe_2As_2$ is calculated to be 0.23 [11] but such calculations for $CaFe_2P_2$ are not yet available. Because of their structural and electronic similarities it is likely that in $CaFe_2P_2$ a mass enhancement of $1 + \lambda_{e-\mathrm{ph}} \sim 1.23$ could be due to a conventional electron-phonon coupling, but other effects could also be important [19]. The further anisotropic mass enhancement due to many-body interactions observed in LaFePO and possibly in $SrFe_2P_2$ could have another origin and may be related to the nesting of the Fermi surface. The mean free paths, ℓ, of the minimum electronic orbit is a factor of 2 larger than that of large hole sheet and of the maximum electronic orbit. This suggests both anisotropy in scattering between electron and holes but also along k_z, as also observed in $SrFe_2P_2$ and LaFePO [8,9].

In the case of the superconducting LaFePO and $SrFe_2P_2$ [8,9] the energies in the band structure were shifted in opposite direction for the electron and hole pockets to match up the experimental data. These asymmetric band shifts are suggested to result from geometric nesting [21]; as no band shifts were necessary in the present measurements ($\sim \pm 10$ meV) it would imply the absence of nesting in $CaFe_2P_2$ (or the lack of long-range order in the CT phase of $CaFe_2As_2$ [22].)

In conclusion, we have experimentally determined the Fermi surface of $CaFe_2P_2$ which is closely related to the collapsed tetragonal phase of $CaFe_2As_2$. We find that the Fermi surface is composed of a single highly dispersive electron cylinder at the zone corners and a large three-dimensional hole surface. The mass enhancement due to many-body interactions is isotropic ($\sim$1.5) and may be dominated by the electron-phonon coupling. The features of this Fermi surface which does not fulfill a nesting condition is likely to be shared by the nonmagnetic CT phase of $CaFe_2As_2$ and other ternary pnictides with reduced c/a ratio and may explain why superconductivity is absent in such a state.

We thank M. Haddow and E. Yelland for technical support. We acknowledge financial support from the Royal Society and EPSRC. Work at Stanford was supported by the U.S. DOE, Office of Basic Energy Sciences, DE-AC02-76SF00515. Work performed at the NHMFL in Tallahassee, was supported by NSF Cooperative Agreement No. DMR-0654118, by the State of Florida, and by the DOE.

[1] P. Alireza *et al.*, J. Phys. Condens. Matter **21**, 012208 (2009).
[2] W. Yu *et al.*, Phys. Rev. B **79**, 020511(R) (2009).
[3] M. S. Torikachvili, S. L. Bud'ko, N. Ni, and P. C. Canfield, Phys. Rev. Lett. **101**, 057006 (2008).
[4] A. Kreyssig *et al.*, Phys. Rev. B **78**, 184517 (2008).
[5] D. A. Tompsett and G. G. Lonzarich, arXiv:0902.4859.
[6] Y.-Z. Zhang *et al.*, arXiv:0812.2920.
[7] J. G. Analytis *et al.*, arXiv:0902.1172.
[8] A. I. Coldea *et al.*, Phys. Rev. Lett. **101**, 216402 (2008).
[9] J. G. Analytis *et al.*, arXiv:0904.2405.
[10] E. Gustenau, P. Herzig, and A. Neckel, J. Solid State Chem. **129**, 147 (1997).
[11] T. Yildirim, Phys. Rev. Lett. **102**, 037003 (2009).
[12] P. Blaha, K. Schwarz, G. K. H. Madsen, D. Kvasnicka, and J. Luitz, *WIEN2K, An Augmented Plane Wave + Local Orbitals Program for Calculating Crystal Properties* (Karlheinz Schwarz, Techn. Universität Wien, Austria, 2001).
[13] $a = 3.855$ Å, $c = 9.985$ Å, and $z_P = 0.3643$ for $CaFe_2P_2$ [14], $a = 3.8915$ Å, $c = 11.690$ Å, and $z_P = 0.372$ for $CaFe_2As_2$ [4], and $a = 3.978$ Å, $c = 10.607$ Å, and $z_P = 0.3663$ for $CaFe_2As_2$ in the CT phase ($p = 0.63$ GPa) [4].
[14] A. Mewis, Z. Naturforsch. B **35**, 141 (1980).
[15] The x-ray diffraction shows that sample A contains a single domain with a ($\sim$1°) mosaic spread and about 1% of another phase misaligned in the (ac) plane.
[16] J. E. Craven, Phys. Rev. **182**, 693 (1969).
[17] A. Kimber *et al.*, Nature Mater. **8**, 471 (2009).
[18] D. Schoenberg, *Magnetic Oscillations in Metals* (Cambridge University Press, London, 1984).
[19] Many-body interactions could be responsible for a further enhancement of the electron-phonon interaction due to the strong polarization of pnictogen ions [20].
[20] M. Kulic and A. Haghighirad, arXiv:0904.3512.
[21] L. Ortenzi *et al.*, arXiv:0903.0315.
[22] A. I. Goldman *et al.*, Phys. Rev. B **79**, 024513 (2009).